Table 2.2.5.1. *The distance displacement (in mm) measured on the film versus angular setting error of the crystal for a screenless precession ($\bar{\mu} = 5°$) setting photograph*

Angular correction, ε, in degrees and minutes	Δ r.l.u	Distance displacement (mm) for three crystal-to-film distances		
		60 mm	75 mm	100 mm
0	0	0	0	0
15′	0.0175	1.1	1.3	1.8
30′	0.035	2.1	2.6	3.5
45′	0.0526	3.2	4.0	5.3
60′	0.070	4.2	5.3	7.0
1° 15′	0.087	5.2	6.5	8.7
1° 30′	0.105	6.3	7.9	10.5
1° 45′	0.123	7.4	9.2	12.3
2°	0.140	8.4	10.5	14.0

Alternatively, $\Delta = \delta/D \simeq \sin 4\varepsilon$ can be used if ε is small [from equation (2.2.5.1)].

Notes

(1) A value of $\bar{\mu}$ of 5° is assumed although there is a negligible variation in ε with $\bar{\mu}$ between 3° (typical for proteins) and 7° (typical for small molecules).

(2) Crystal-to-film distances on a precession camera are usually settable at the fixed distance $D = 60$, 75, and 100 mm.

(3) This table should be used in conjunction with Fig. 2.2.5.1.

(4) Values of ε are given in intervals of 5′ as this is convenient for various goniometer heads which usually have verniers in 5′, 6′ or 10′ units. The vernier on the spindle of the precession camera is often in 2′ units.

relative to the zero-layer photograph. This effect can be eliminated by initial translation of the cassette by $D \tan \mu$.

2.2.5. Precession geometry

The main book dealing with the precession method is that of Buerger (1964).

2.2.5.1. *General*

The precession method is used to record an undistorted representation of a single plane of relp's and their associated intensities. In order to achieve this, the crystal is carefully set so that the plane of relp's is perpendicular to the X-ray beam. The normal to this plane, the zone axis, is then precessed about the X-ray-beam axis. A layer-line screen allows only relp's of the plane of interest to pass through to the film. The motion of the crystal, screen, and film are coupled together to maintain the coplanarity of the film, screen, and zone.

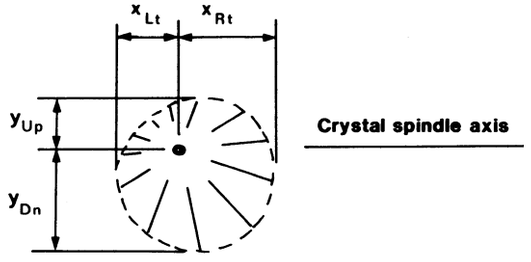

Fig. 2.2.5.1. The screenless precession setting photograph (schematic) and associated mis-setting angles for a typical orientation error when the crystal has been set previously by a monochromatic still or Laue.

2.2.5.2. *Crystal setting*

Setting of the crystal for one zone is carried out in two stages. First, a Laue photograph is used for small molecules or a monochromatic still for macromolecules to identify the required zone axis and place it parallel to the X-ray beam. This is done by adjustment to the camera-spindle angle and the goniometer-head arc in the horizontal plane. This procedure is usually accurate to a degree or so. Note that the vertical arc will only rotate the pattern around the X-ray beam. Second, a screenless precession photograph is taken using an angle of ~ 7–$10°$ for small molecules or 2–3° for macromolecules. It is better to use unfiltered radiation, as then the edge of the zero-layer circle is easily visible. Let the difference of the distances from the centre of the pattern to the opposite edges of the trace in the direction of displacement be called $\delta = D\Delta$ so that for the horizontal goniometer-head arc and the dial: $\delta_{\rm arc} = x_{\rm Rt} - x_{\rm Lt}$ and $\delta_{\rm dial} = y_{\rm Up} - y_{\rm Dn}$ (Fig. 2.2.5.1). The corrections ε to the arc and camera spindle are given by

$$\Delta = \frac{\delta}{D} = \frac{\sin 4\varepsilon \cos \bar{\mu}}{\cos^2 2\varepsilon - \sin^2 \bar{\mu}} \text{ in r.l.u.,} \qquad (2.2.5.1)$$

where D is the crystal-to-film distance and $\bar{\mu}$ is the precession angle.

It is possible to measure δ to about 0.3 mm ($\delta = 1$ mm corresponds to 14′ error for $D = 60$ mm and $\bar{\mu} \simeq 7°$ [Table 2.2.5.1, based on *IT* II (1959, p. 200)].

2.2.5.3. *Recording of zero-layer photograph*

Before the zero-layer photograph is taken, an Nb filter (for Mo $K\alpha$) or an Ni filter (for Cu $K\alpha$) is introduced into the X-ray beam path and a screen is placed between the crystal and the film at a distance from the crystal of

$$s = r_s \cot \bar{\mu}, \qquad (2.2.5.2)$$

where r_s is the screen radius. Typical values of $\bar{\mu}$ would be 20° for a small molecule with Mo $K\alpha$ and 12–15° for a protein with Cu $K\alpha$. The annulus width in the screen is chosen usually as 2–3 mm for a small molecule and 1–2 mm for a macromolecule. A clutch slip allows the camera motor to be disengaged and the precession motion can be executed under hand control to check for fouling of the goniometer head, crystal, screen or film cassette; s and r_s need to be selected so as to avoid this happening. The zero-layer precession photograph produced has a radius of $2D \sin \bar{\mu}$ corresponding to a resolution limit $d_{\rm min} = \lambda/2 \sin \bar{\mu}$. The distance between spots A is related to the reciprocal-cell parameter a^* by the formula

$$a^* = \frac{A}{D}. \qquad (2.2.5.3)$$

2.2.5.4. *Recording of upper-layer photographs*

The recording of upper-layer photographs involves isolating the net of relp's at a distance from the zero layer of $\zeta_n = n\lambda/b$, where b is the case of the b axis antiparallel to the X-ray beam. In order to determine ζ_n, it is generally necessary to record a cone-axis photograph. If the cell parameters are known, then the camera settings for the upper-level photograph can be calculated directly without the need for a cone-axis photograph.

In the upper-layer precession photograph, the film is advanced towards the crystal by a distance

$$D\zeta_n \qquad (2.2.5.4)$$

and the screen is placed at a distance

$$s_n = r_s \cot \bar{\nu}_n = r_s \cot \cos^{-1}(\cos \bar{\mu} - \zeta_n). \quad (2.2.5.5)$$

The resulting upper-layer photograph has outer radius

$$D(\sin \bar{\nu}_n + \sin \bar{\mu}) \quad (2.2.5.6)$$

and an inner blind region of radius

$$D(\sin \bar{\nu}_n - \sin \bar{\mu}). \quad (2.2.5.7)$$

2.2.5.5. *Recording of cone-axis photograph*

A cone-axis photograph is recorded by placing a film enclosed in a light-tight envelope in the screen holder and using a small precession angle, *e.g.* 5° for a small molecule or 1° for a protein. The photograph has the appearance of concentric circles centred on the origin of reciprocal space, provided the crystal is perfectly aligned. The radius of each circle is

$$r_n = s \tan \bar{\nu}_n, \quad (2.2.5.8)$$

where

$$\cos \bar{\nu}_n = \cos \bar{\mu} - \zeta_n. \quad (2.2.5.9)$$

Hence, $\zeta_n = \cos \bar{\mu} - \cos \tan^{-1}(r_n/s)$.

2.2.6. Diffractometry

The main book dealing with single-crystal diffractometry is that of Arndt & Willis (1966). Hamilton (1974) gives a detailed treatment of angle settings for four-circle diffractometers. For details of area-detector diffractometry, see Howard, Nielsen & Xuong (1985) and Hamlin (1985).

2.2.6.1. *General*

In this section, we describe the following related diffractometer configurations:

(*a*) normal-beam equatorial geometry [ω, χ, φ option or ω, κ, φ (kappa) option];

(*b*) fixed $\chi = 45°$ geometry with area detector.

(*a*) is used with single-counter detectors. The kappa option is also used in the television area-detector system of Enraf–Nonius (the FAST). (*b*) is used with the multiwire proportional chamber, XENTRONICS, system. (FAST is a trade name of Enraf–Nonius; XENTRONICS is a trade name of Siemens.)

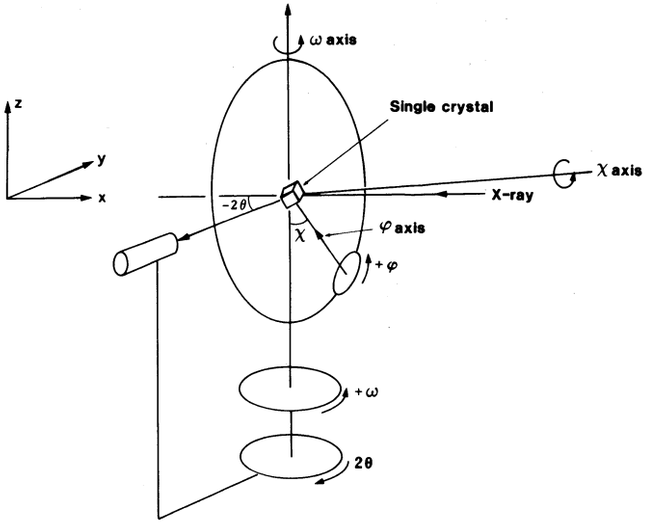

Fig. 2.2.6.1 Normal-beam equatorial geometry: the angles ω, χ, φ, 2θ are drawn in the convention of Hamilton (1974).

The purpose of the diffractometer goniostat is to bring a selected reflected beam into the detector aperture or a number of reflected beams onto an area detector of limited aperture (*i.e.* an aperture that does not intercept all the available diffraction spots at one setting of the area detector) [see Hamlin (1985, p. 431), for example].

Since the use of electronic area detectors is now increasingly common, the properties of these detectors that relate to the geometric prediction of spot position will be described later.

The single-counter diffractometer is primarily used for small-molecule crystallography. In macromolecular crystallography, many relp's are almost simultaneously in the diffraction condition. The single-counter diffractometer was extended to five separate counters [for a review, see Artymiuk & Phillips (1985)], then subsequently to a multi-element linear detector [for a review, see Wlodawer (1985)]. Area detectors offer an even larger aperture for simultaneous acquisition of reflections [Hamlin *et al.* (1981), and references therein].

Large-area on-line image-plate systems are now available commercially to crystallographers, whereby the problem of the limited aperture of electronic area detectors is circumvented and the need for a goniostat is relaxed so that a single axis of rotation can be used. Systems like the R-AXISIIc (Rigaku Corporation) and the MAR (MAR Research Systems) fall into this category, utilizing IP technology and an on-line scanner. A next generation of device beckons, involving CCD area detectors. These offer a much faster duty cycle and greater sensitivity than IP's. By tiling CCD's together, a larger-area device can be realized. However, it is likely that these will be used in conjunction with a three-axis goniostat again, except in special cases where a complete area coverage can be realized.

2.2.6.2. *Normal-beam equatorial geometry*

In normal-beam equatorial geometry (Fig. 2.2.6.1), the crystal is oriented specifically so as to bring the incident and reflected beams, for a given relp, into the equatorial plane. In this way, the detector is moved to intercept the reflected beam by a single rotation movement about a vertical axis (the 2θ axis). The value of θ is given by Bragg's law as $\sin^{-1}(d^*/2)$. In order to bring $\mathbf{d}^*$ into the equatorial plane (*i.e.* the Bragg plane into the meridional plane), suitable angular settings of a three-axis goniostat are necessary. The convention for the sign of the angles given in Fig. 2.2.6.1 is that of Hamilton (1974); his choice of sign of 2θ is adhered to despite the fact that it is left-handed, but in any case the signs of ω, χ, φ are standard right-handed. The

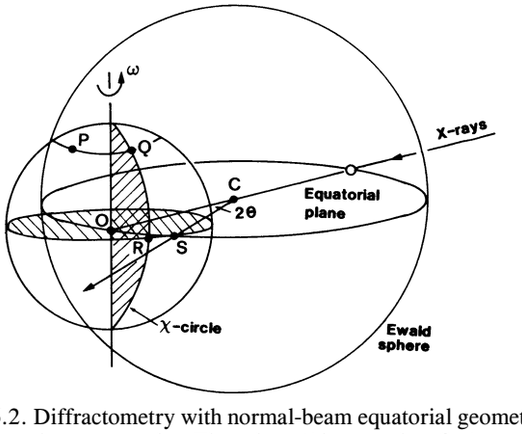

Fig. 2.2.6.2. Diffractometry with normal-beam equatorial geometry and angular motions ω, χ and φ. The relp at *P* is moved to *Q via* φ, from *Q* to *R via* χ, and *R* to *S via* ω. From Arndt & Willis (1966). In this specific example, the φ axis is parallel to the ω axis (*i.e.* $\chi = 0°$).